



Energy, Mines and
Resources Canada

Énergie, Mines et
Ressources Canada

CANMET

Canada Centre
for Mineral
and Energy
Technology

Centre canadien
de la technologie
des minéraux
et de l'énergie

CATALYTIC GASIFICATION OF CHAR FROM HYDROCRACKED PITCH

M.V.C. Sekhar and M. Ternan

Catalysis Section
Synthetic Fuels Research Laboratory

March 1979

ERP/ERL 79-47 (J)

ENERGY RESEARCH PROGRAM
ENERGY RESEARCH LABORATORIES
REPORT ERP/ERL 79-47 (J)

Catalytic Gasification of Char from Hydrocracked Pitch

by

M.V.C. Sekhar and M. Ternan

Energy Research Laboratories

Department of Energy, Mines and Resources Canada

Ottawa, Ontario, K1A 0G1

ABSTRACT

Gasification of hydrocracked pitch (vacuum residuum) was performed non-catalytically and with K_2CO_3 and V_2O_5 catalysts. In agreement with studies of many other workers K_2CO_3 was found to enhance the gasification rate. In contrast V_2O_5 was found to inhibit gasification when compared to the non-catalytic rate. X-ray photoelectron spectra were obtained on both catalysts and on catalyst-pitch residues. They indicated that K_2CO_3 does not exist under reaction conditions. This experimental finding suggests that some of the catalytic gasification mechanisms recently reported in the literature may be incorrect. In this work both catalysis and inhibition during gasification have been explained in terms of three effects, reaction at carbon edge planes, intercalation of the catalyst or inhibitor, and electron transfer. Potassium donates its outer electron to the pi-electron clouds associated with the carbon layers. Extra electrons facilitate the formation of an unstable reaction intermediate which leads to the evolution of carbon monoxide. The vacant d-orbitals in vanadium stabilize pi-electrons in the carbon layers thereby making carbon monoxide evolution less likely. Thus, opposite extremes of a single effect account for both catalysis and inhibition.

Catalytic Gasification of Char from Hydrocracked Pitch

by

M.V.C. Sekhar and M. Ternan

Energy Research Laboratories

Department of Energy Mines and Resources

Ottawa, Ontario, Canada, K1A 0G1

Gasification of coal, coke and other carbonaceous materials to produce synthesis gas has received considerable attention in recent years. The carbonaceous material gasified in this study and referred to as pitch was the vacuum residuum by-product produced during hydrocracking of Alberta oil sands bitumen. It contains high concentrations of sulphur, vanadium, iron, nickel and other heavy metals. As a result alternate uses of the pitch such as direct burning and cokemaking are not attractive. Gasification however, is of interest because the synthesis gas produced can be processed further to yield hydrogen or can be used directly as a low-BTU industrial fuel. Each of these products could be used on site in an oil sands upgrading facility. The present work describes the effects of some well known catalysts on the gasification of pitch.

EXPERIMENTAL

The pitch used in this study was the portion of the liquid product boiling above 525°C obtained by thermally hydrocracking Athabasca bitumen in a pilot plant reactor. Its properties have been described previously [1]. The Athabasca bitumen was obtained from Great Canadian Oil Sands Ltd., at Fort McMurray, Alberta. The chemicals used as catalysts were analytical grade reagents and were used without further purification.

A semi-batch reaction system was used to study the gasification rate [1]. Samples of pitch mixed with the powdered catalyst were placed in a cylindrical quartz basket, which was suspended from the weighing mechanism of a Cahn RG Electrobalance. A stream of dry nitrogen flowed through the chamber containing the weighing mechanism and entered the top of the hangdown tube containing the pitch sample. Nitrogen saturated with

water vapour (the gasification reactant) flowed directly into the hangdown tube which was surrounded by a tubular furnace. Both the sample weight and the interior temperature of the hangdown tube were monitored continuously.

In a typical experiment the sample was initially heated in an atmosphere of flowing nitrogen until no further weight loss was observed. Next the furnace temperature was lowered to the desired value, usually between 700°C and 1200°C. The reaction between carbon and water vapour was then initiated by introducing a stream of nitrogen (100 mL/min) saturated with water vapor at room temperature (23 mm, 3.1 kPa). A Wilks Infrared Analyzer was used to monitor continuously the carbon monoxide level in the reaction products. The products were also analyzed at intervals by gas chromatography. In one experiment an Horiba model PIR 2000 infrared analyzer was used to continuously monitor the carbon dioxide. The x-ray photoelectron spectra were obtained with a Perkin Elmer model 548 spectrometer using a magnesium anode at 10 KeV and 40 ma with a pass energy of 50 eV.

RESULTS AND DISCUSSION

The gasification of a complex multi-component solid such as pitch involves a number of different reactions, which might be occurring simultaneously. Previously we noted that as the pitch sample is brought to temperatures at which gasification rates become measureable, considerable pyrolytic decompositions occurred causing the formation of volatile gaseous and liquid products [1]. Some of the pyrolysis products detected during pyrolysis included methane, carbon monoxide and hydrogen. In order to separate the gasification and pyrolysis reactions the pitch samples were pyrolyzed before being contacted with steam. The solid char remaining after completion of pyrolytic reactions consisted essentially of carbon with small amounts residual hydrogen and sulphur.

In the absence of any gasification agent other than steam, the reactions that need to be considered are:



The last reaction, between carbon and product hydrogen is known to proceed at slow rates at atmospheric pressures. Further, it's equilibrium constant has a value of 0.3 atmospheres (30 kPa) at 900°C and decreases with increasing temperature. Methane formation can be expected only at relatively low temperatures and high pressures. The CO-shift reaction (Eq 2) is weakly exothermic and is unaffected by pressure. However, it's equilibrium constant also decreases with increasing temperatures approaching a value of 2 at 900°C. Since most experiments in this study were conducted at temperatures above 800°C, this reaction can be neglected.

The only detectable products of gasification were carbon monoxide and hydrogen. It is unlikely that any carbon dioxide formed via reaction 2 would have completely reacted with the carbon to form CO (viz Eq 3). The absence of any CO₂ in the product analysis thus confirms the unimportance of reactions 2 and 3, leaving reaction 1 as the only reaction occurring in the present system.

Two types of catalysts were evaluated in this investigation. One was K₂CO₃, the well known gasification catalyst which has been found to be active with a variety of carbonaceous materials including several types of coal chars [2-7]. The other catalyst was V₂O₅, an oxidation-reduction catalyst commonly used for the oxidation of hydrocarbon compounds.

Typical experimental data showing the weight of the char as a function of time under isothermal conditions are given in Figure 1. The relationship between sample weight *w* and time *t* is linear during the initial stages of the reaction. With time, the weight slowly levels off approaching a constant value for a given temperature.

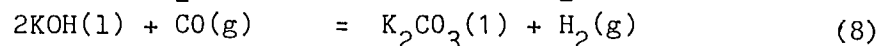
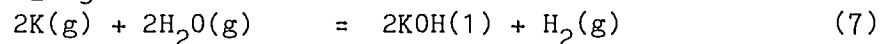
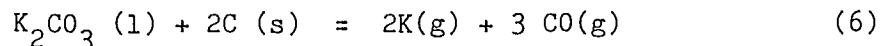
A simple model for reaction 1 has been proposed by Van Heek et al [8]. This model assumes that the reaction rate depends only on the amount of char present and that the reaction is first order with respect to the solid phase. This assumption is appropriate for the present study since the extent of steam decomposition was low and therefore the steam concentration could be considered to remain constant.

The reaction rate is then given by:

$$-\frac{d w}{d t} = k w \quad (5)$$

where w represents the weight of the char remaining in the reaction at time t and k the overall rate constant. The slope of the linear segment of the curve in Figure 1 corresponds to the initial rate for the corresponding temperature. These weight-loss rates are plotted as a function of $1/T$ in Figure 2 where T is in degrees Kelvin. The uncatalyzed reaction had a measurable rate at 800°C and above with an apparent activation energy of 145 kJ/mol. Addition of 7 wt% of potassium carbonate increases the gasification rate and decreases the apparent activation energy as shown in Table 1. Vanadium pentoxide on the other hand acts as an inhibitor and increases the apparent activation energy of the reaction.

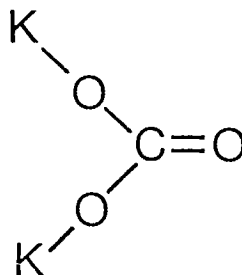
The action of alkali metal catalysts during gasification has been reviewed recently by Wen [9]. Explanations [6,7] for the superior activity of K_2CO_3 involve the following cycle of reactions, (6) the initial reduction of the alkali carbonate to alkali metal, (7) reaction with steam to form alkali hydroxide, and (8) reaction with carbon monoxide or carbon dioxide to regenerate the alkali carbonate.



The difficulty with explanations of this type is that the first reaction Equation 6 is thermodynamically unfavorable at the gasification conditions employed. However it has been noted [7] that this reaction will take place if the concentrations of the reaction products (alkali metal and carbon monoxide) are maintained at very low levels.

In an attempt to examine the chemical state of the catalyst, several samples were analyzed by x-ray photoelectron spectroscopy. Figure 3 shows oxygen 1s spectra of K_2CO_3 samples. The O 1s spectrum (curve A) for K_2CO_3 shows that the maximum peak height occurs at a binding energy of 536.7 eV and that a shoulder occurs at approximately 539 eV. These

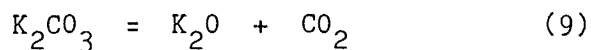
binding energies can be related to the following structure of K_2CO_3 .



The maximum peak height can be associated with the oxygen ions which are adjacent to the potassium ions (oxygen with single bonds). The shoulder can be associated with the oxygen ions which are not adjacent to potassium ions (oxygen with double bonds). The intensity of the XPS signal from double bonded oxygen should be one half that of single bonded oxygen.

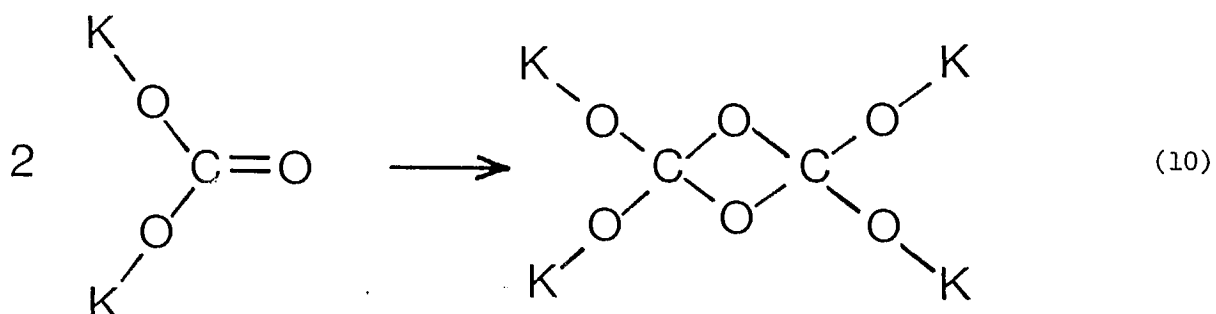
As expected curve A in Figure 3 verifies this ratio. It is reasonably to suggest that the area under the peak at 536.7 eV (single bonded oxygen) is twice as large as the area under the shoulder at 539 eV (double bonded oxygen).

Experiments were also performed by heating the K_2CO_3 catalyst to temperatures at which the gasification reaction becomes thermodynamically feasible. Solid samples obtained after heating K_2CO_3 for 2 hours at $600^\circ C$, in flowing dry nitrogen (curve B), in a flowing steam-nitrogen mixture (curve C), and in flowing dry nitrogen when the K_2CO_3 had been mixed with pitch, all produced spectra which indicated the presence of only one type of oxygen; the oxygen adjacent to the potassium ions. A sample of K_2CO_3 was placed on the microbalance and heated in the presence of flowing dry nitrogen. The loss in weight shown in Figure 4 accounts for less than 10 percent of the original K_2CO_3 . The exit gas contained carbon dioxide but not carbon monoxide. The weight loss was insufficient for complete conversion of K_2CO_3 via reaction 9

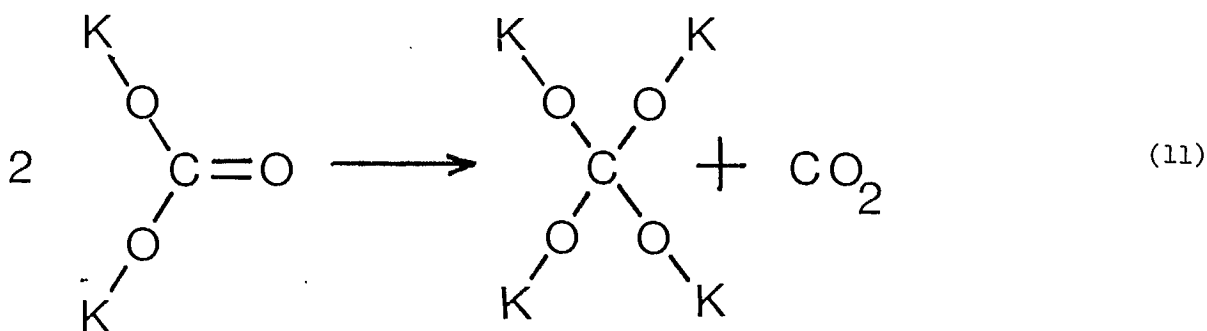


to have occurred. However curve B in Figure 3 indicates that complete conversion of K_2CO_3 did occur since only one type of oxygen is present after heating.

The formation of a dimer as in reaction 10



would explain the absence of double bonded oxygen without requiring a weight loss. Weight loss plus the evolution of carbon dioxide could be explained by either reaction 9 or 11



Equations 10 and 11 may be helpful for illustrative purposes.

However it is also plausible that K_2CO_3 is converted to an ionic structure in which all the oxygen ions are adjacent to potassium ions.

The XPS spectra for potassium and carbon in K_2CO_3 are shown in Figure 5. The potassium peaks indicate that there is probably no change in potassium bonding on heating. This is consistent with reactions 9, 10 and 11. For curves A, B and C, both the potassium and carbon peaks in Figure 5 are at higher binding energies than those normally assigned to potassium (292.9 eV) and to carbon (284.6 eV). This is due to sample charging. The peaks are at lower binding energies in curve D because this sample contained a large amount of char (originating from the pitch), which is a reasonably good electrical conductor. Hence less sample charging would be expected.

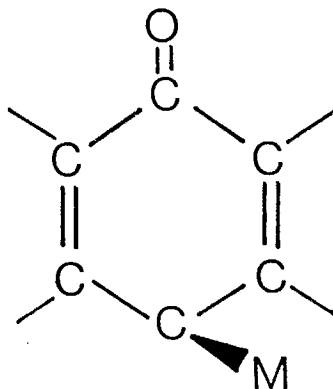
The information on weight loss and carbon dioxide evolution in Figure 4 combined with the presence of a single type oxygen in Figure 3 indicates that K_2CO_3 as such will not exist at gasification temperatures. This suggests that the function of the catalyst may be different than that

indicated in previously suggested mechanisms, reactions 6 to 8.

Figure 6 shows the oxygen and vanadium spectra of the V_2O_5 catalyst. No chemical changes were produced by heating in nitrogen. However heating V_2O_5 in the presence of steam (curve C) produced a distinct shoulder on the oxygen peak, indicating a second type of oxygen. The presence of steam did not change the position of the vanadium peak or the main oxygen peak. Furthermore the vanadium to oxygen peak height ratio in curve C (using the peak height of the main oxygen peak) is similar to the peak height ratio in curves A and B. This suggests that the oxygen shoulder is caused by water which has entered the V_2O_5 lattice. It is not surprising that the binding energy of oxygen electrons in water is different from that in V_2O_5 . Heating V_2O_5 when mixed with pitch, curve D, produced two changes. The vanadium signal at 517.7 eV disappeared and the oxygen 0 1s signal shifted to a higher binding energy. The shift in binding energy is not caused by differences in sample charging since the C 1s signals for curves C and D both had peak maximums at 284.8eV.

It has already been noted that several previous studies have attempted to explain the catalytic effect of K_2CO_3 . We are not aware of any previous explanations for inhibition of V_2O_5 . In principle both effects should be caused by opposite extremes of the same phenomenon. One possible explanation would be electron transfer (donors and acceptors).

Long and Sykes [10] indicated that electrons from the carbonaceous solid are transferred to, or form extra bonds with, the catalyst (or inhibitor). They reasoned that the loss of electrons from the carbonaceous solid would weaken the carbon-carbon bonds and facilitate the evolution of CO as shown,



where M is the catalyst (or inhibitor).

The inhibition and catalytic effects observed in this work can be explained in terms of three effects, reaction at carbon edge planes, inter-

calation of the catalyst or inhibitor, and electron transfer.

The char formed from the hydrocracked pitch is different from graphite in that it contains an appreciable amount of heteroatoms, primarily sulphur, as well as some residual hydrogen [1]. Some types of amorphous carbonaceous solids (carbon blacks, pyrolytic carbons) have been described as turbostratic structures. They are 20-25 nm diameter crystallites [11] having parallel planes of carbon atoms. The spacing [12] between layers is larger in turbostratic structures (0.344 nm) than in graphite (0.3354 nm). A suitable model for our chars would therefore be small domains consisting of parallel layers of carbon atoms containing imperfections resulting from heteroatoms (S, H, N, O, metals). Each of these domains would be stacked at an angle with respect to its neighbors.

Reaction rates on planes composed of the edges of carbon layers are known to be orders magnitude larger than those on the base planes of carbon layers [13]. Otto, Bartosiewicz and Shelef [14] have discussed the steam-carbon reaction in terms of carbon atoms at edge planes and at basal planes. These results suggest that most of the reactions will occur at edge planes on the exterior of the domains.

The K_2CO_3 catalyst [9] and V_2O_5 inhibitor [15] are known to intercalate between the layers of the carbon atoms. The concentration of intercalated species decreases with increasing temperature and is quite small at gasification temperatures [9]. When intercalation compounds are decomposed the resulting residue compounds always contain a small amount of the intercalated species. Impurities in residue compounds are considered to be located in holes and imperfections in the layer structure [16]. This suggests that a major portion of the catalyst will be situated at edge plane defects on the exterior of the domains. Hennig [13] has commented that catalysis only occurs when the catalyst contacts the edge surfaces of the carbon layers.

Figure 7 shows the intercalation of a catalyst (or inhibitor) species, M, between two carbon layers at the edge of a domain. The carbon atoms form hexagons in each layer. In Figure 7 the intersection of the lines indicate the locations of carbon atoms. The layers do not stack directly on top of one another. This is indicated by the dashed hexagon. It is a projection from the second layer onto the first layer. Croft [17,18] has stated that two electrons of the graphite are transferred to

the incompletely filled electron shells of the intercalated species, M. The details of the concepts of Croft and of Long and Sykes [10] must be changed substantially to explain K_2CO_3 catalysis and V_2O_5 inhibition.

The explanation now being offered employs electronic concepts. Following Long and Sykes, the evolution of carbon monoxide is considered to be the rate limiting step. When potassium is the intercalated species, its outermost electron is added to the pi-electrons in one of the carbon planes. This extra electron allows molecular rearrangements to occur more readily and is responsible for catalysis of carbon-carbon bond cleavage. Conversely when vanadium is the intercalated species pi electrons from the carbon layers may be shared with or transferred to unfilled vanadium d-orbitals. The electron sharing, similar to crystal field stabilization makes molecular rearrangements more difficult. It effectively withdraws electrons from the carbon layers and causes inhibition of carbon-carbon bond cleavage.

This process is illustrated pictorially in Figure 8. Figure 8A shows the sigma and pi bonds between an oxygen atom and one of the carbon atoms in an edge surface of a carbon layer. The dotted lines represent the pi electrons above and below the layer of carbon atoms. The sigma bond is between the axes of carbon and oxygen. The carbon-oxygen pi bond is shown in the same planes as the pi electrons of the carbon layers. In Figure 8B, each atom of potassium catalyst, K, is able to contribute one electron to the pi electron clouds of the carbon layers. One can speculate that extra electrons assist in the formation of a second pi bond between the oxygen and carbon. This hypothetical reaction intermediate in which the carbon atom has an abnormal number of bonds would be unstable, allowing easier cleavage of the carbon-carbon bonds, and the evolution of carbon monoxide as shown in Figure 8C.

The presence of vanadium as an intercalated species would have the opposite effect. Presumably some of the pi electrons in carbon layers would be stabilized by interaction with the vacant d-orbitals in vanadium. As a result they would be less likely to form a second pi bond between the oxygen and carbon atoms. The possibility of forming a second pi bond would be even lower when vanadium is present than when carbon layers contained no intercalated species. Thus catalysis and inhibition can be explained by potassium acting as an electron donor and vanadium acting as an electron acceptor.

The findings of this work can be summarized as follows. Experimen-

tal studies on the gasification of char from hydrocracked pitch have shown K_2CO_3 to be a catalyst and V_2O_5 to be an inhibitor. Electronic concepts have been invoked to explain both effects. Potassium donates electrons to the pi-electron clouds associated with the carbon layers. This facilitates the evolution of CO. In contrast vanadium effectively removes pi-electrons, thereby making CO evolution less likely.

REFERENCES

1. Sekhar, M.V.C. and Ternan, M., 1979. Pyrolysis of pitch derived from hydrocracked Athabasca bitumen, *Fuel*, 58:92.
2. Peter, S., Woyke, G. and Baumgartel, G., 1978. Catalytic gasification of coal with high pressure steam, *Int. J. Chem. Eng.*, 18:213.
3. Kayembe, N. and Pulsifer, A.H., 1976. Kinetics and catalysis of the reaction of coal char and steam, *Fuel*, 55:211.
4. Cox, J.L., Sealock, Jr., L.J. and Hoodmaker, F.C., 1975. Sulphur problems in the direct catalytic production of methane from coal-steam reactions, *Energy Sources*, 2:83.
5. Wilks, K.A., 1974. The gasification of coal chars, M.S. Thesis, Chem. Eng. Dept., Case Western Reserve University, Ohio.
6. Veraa, M.J. and Bell, A.T., 1978. Effect of alkali metal catalysts on gasification of coal char, *Fuel*, 57:194.
7. McKee, D.W. and Chatterji, D., 1978. The catalyzed reaction of graphite with water vapour, *Carbon* 16:53.
8. Van Heek, K.H., Juntgen, H. and Peters, W., 1973. Fundamental studies on coal gasification in the utilization of thermal energy from nuclear high temperature reactors, *J. Inst. Fuel*, 46:249.
9. Wen, W.Y., 1980. Mechanisms of alkali metal catalysis in the gasification of coal, char or graphite, *Catal. Rev. - Sci. Eng.*, 22 (1):1.
10. Long, F.J. and Sykes, K.W., 1952. The effect of specific catalysts on the reactions of the steam-carbon system, *Proc. Roy. Soc.* A215:100.
11. Klein, C.A., 1966. Electronic transport in pyrolytic graphite and boron alloys of pyrolytic graphite, in *Chem. Phys., Carbon* (ed. P.L. Walker), Marcel Dekker, New York 2:225.
12. Robert, M.C., Oberlin, M. and Mering, J., 1973. Lamellar reactions in graphitizable carbons, in *Chem. Phys. Carbon* (eds. P.L. Walker and P.A. Thrower), Marcel Dekker, New York 10:141.
13. Hennig, G.R., 1966. "Electron microscopy of reactivity changes near lattice defects in graphite," in *Chem. Phys. Carbon* (ed. P.L. Walker), Marcel Dekker, New York 2:1.

14. Otto, K., Bartosiewicz, L. and Shelef, M., 1979. "Catalytic steam gasification of graphite: Effects of calcium, strontium and barium with and without sulphur," Carbon 17:351.
15. Baker, R.T.K., Thomas, R.B. and Wells, M., 1975. Controlled atmosphere electron microscopy studies of graphite intercalation - The catalytic influence of vanadium and vanadium pentoxide, Carbon 13:141.
16. Rudorff, W., 1959. "Graphite intercalation compounds," in advances in inorganic chemistry and radiochemistry (eds. H.J. Emeleus and A.G. Sharpe), Academic Press, New York, 1:223.
17. Croft, R.C., 1960. "Lamellar compounds of graphite," Quart. Rev. 14 (1):1.
18. Croft, R.C., 1956. "New molecular compounds of the layer lattice type," Austral. J. Chem. 9:194.

TABLE 1

Catalytic Effects in the Char-Water Reaction

Material	Burn-Off Rate at 900°C(mg/g/min)	Apparent Activation Energy (kJ/mol)
Pitch	0.170	145
Pitch + 7% K_2CO_3	0.420	140
Pitch + 7% V_2O_5	0.050	166

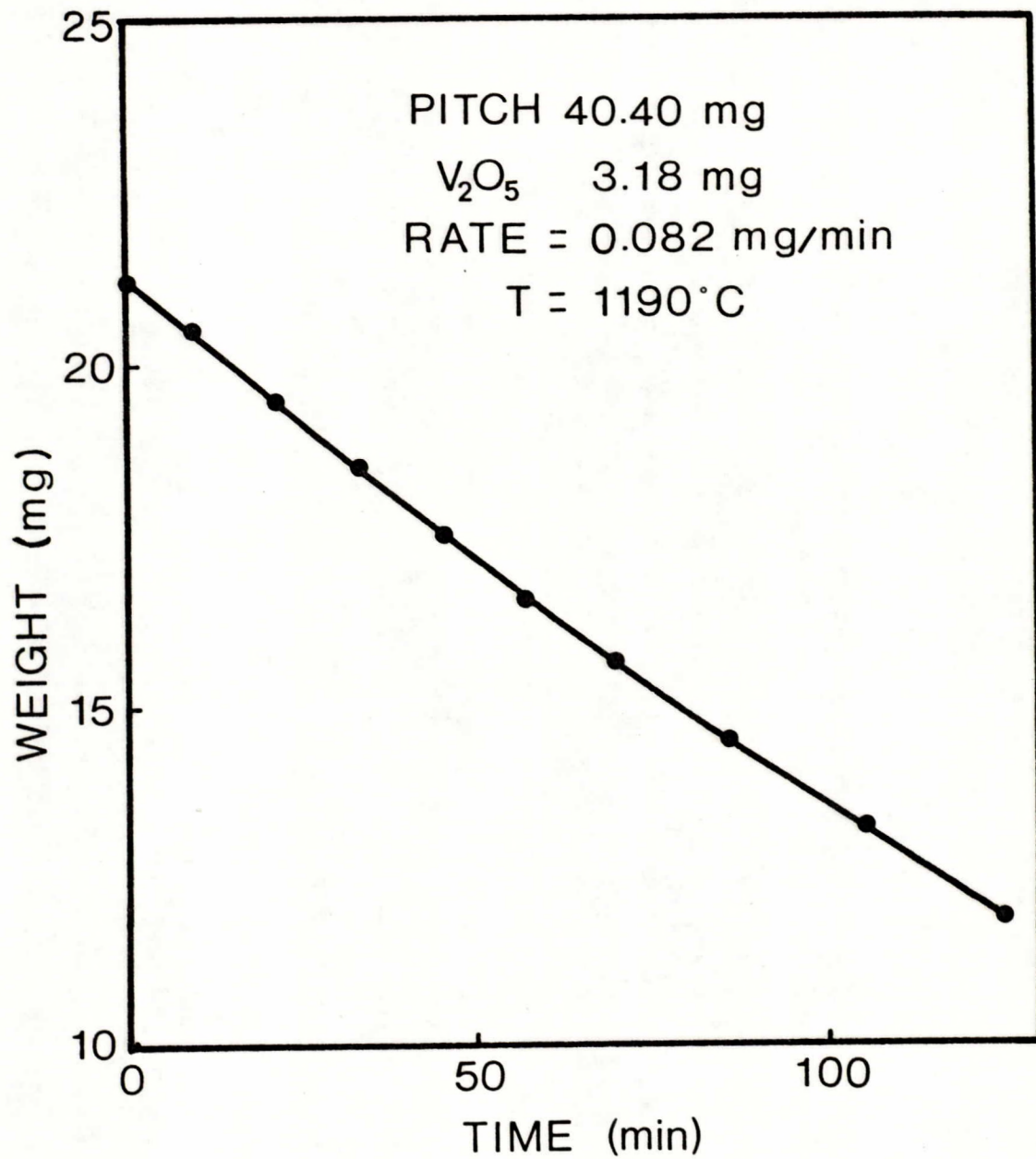
Captions for Figures

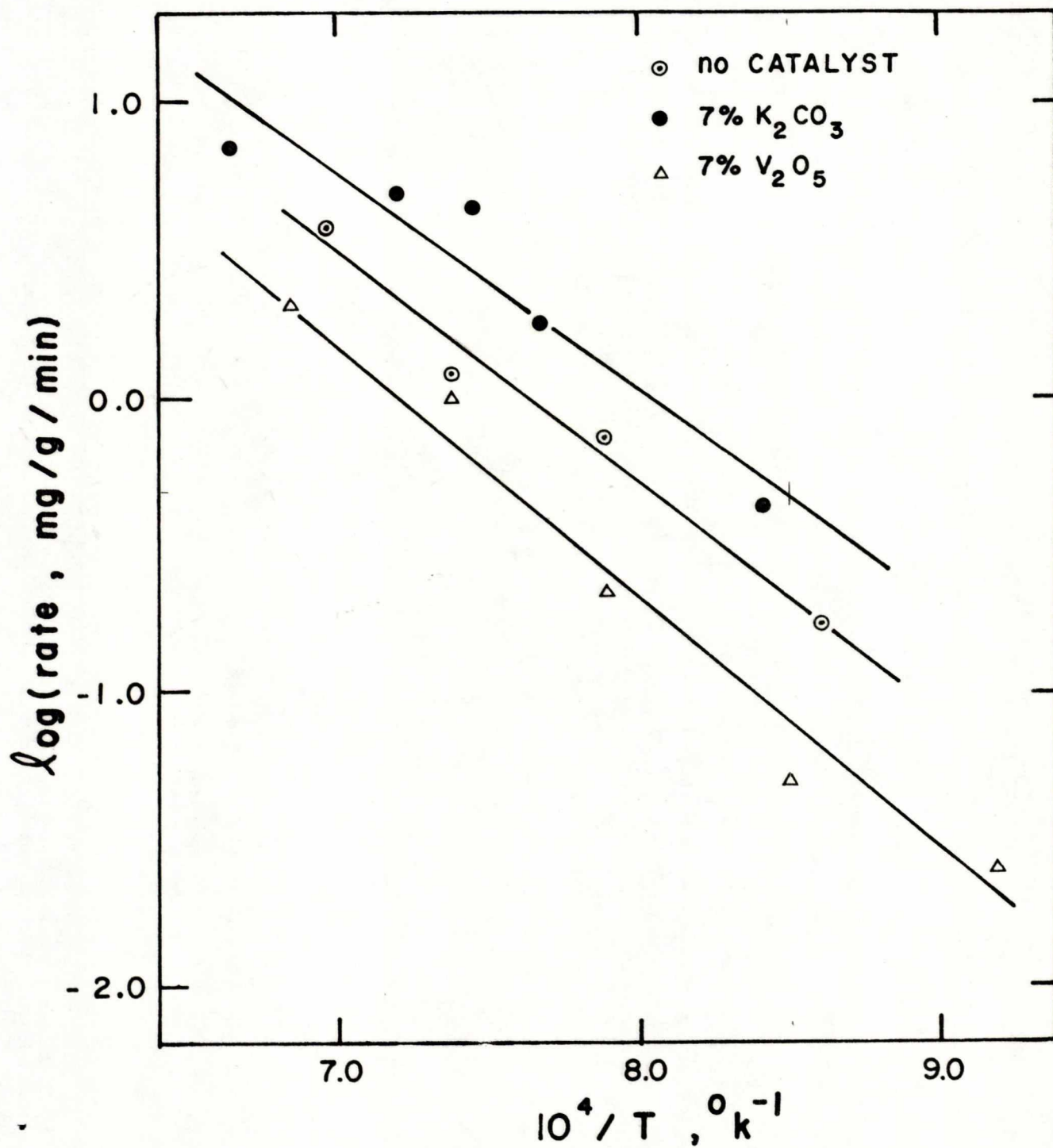
- Figure 1. Weight of Char (mg) Versus Reaction Time (min).
- Figure 2. Common Logarithm of Gasification Rate Versus Inverse Temperature (K^{-1}).
- Figure 3. Relative Intensity of Oxygen (O 1s) Peaks versus Binding Energy (eV) for K_2CO_3 samples. A: K_2CO_3 as received, B: K_2CO_3 after heating in flowing dry nitrogen at $600^\circ C$ for 2 hours, C: K_2CO_3 after heating in a flowing stream of N_2-H_2O at $600^\circ C$ for 2 hours, D: residue from a 25 wt% K_2CO_3 -75 wt% pitch mixture after heating in dry N_2 at $600^\circ C$ for 2 hours.
- Figure 4. Carbon Dioxide Concentration, Carbon Monoxide Concentration, Sample Weight, and Sample Temperature Versus Reaction Time in the Presence of Flowing Dry Nitrogen Using a K_2CO_3 Sample.
- Figure 5. Relative Intensity of Potassium (K 2p) and Carbon (C 1s) Peaks Versus Binding energy (eV) for K_2CO_3 Samples. A: K_2CO_3 as received, B: K_2CO_3 after heating in flowing dry nitrogen at $600^\circ C$ for 2 hours, C: K_2CO_3 after heating in a flowing mixture of N_2-H_2O at $600^\circ C$ for 2 hours, D: residue from a 25 wt% K_2CO_3 -75 wt% pitch mixture after heating in dry N_2 at $600^\circ C$ for 2 hours.
- Figure 6. Relative Intensity of Vanadium (V 2p) and Oxygen (O 1s) Peaks Versus Binding Energy (eV) for V_2O_5 Samples. A: V_2O_5 as received, B: V_2O_5 after heating in flowing dry nitrogen at $600^\circ C$ for 2 hours, and C: V_2O_5 after heating in a flowing mixture of N_2-H_2O at $600^\circ C$ for 2 hours, D: residue from 25 wt% V_2O_5 -75

wt% pitch mixture after heating in dry N_2 at $600^\circ C$ for 2 hours.

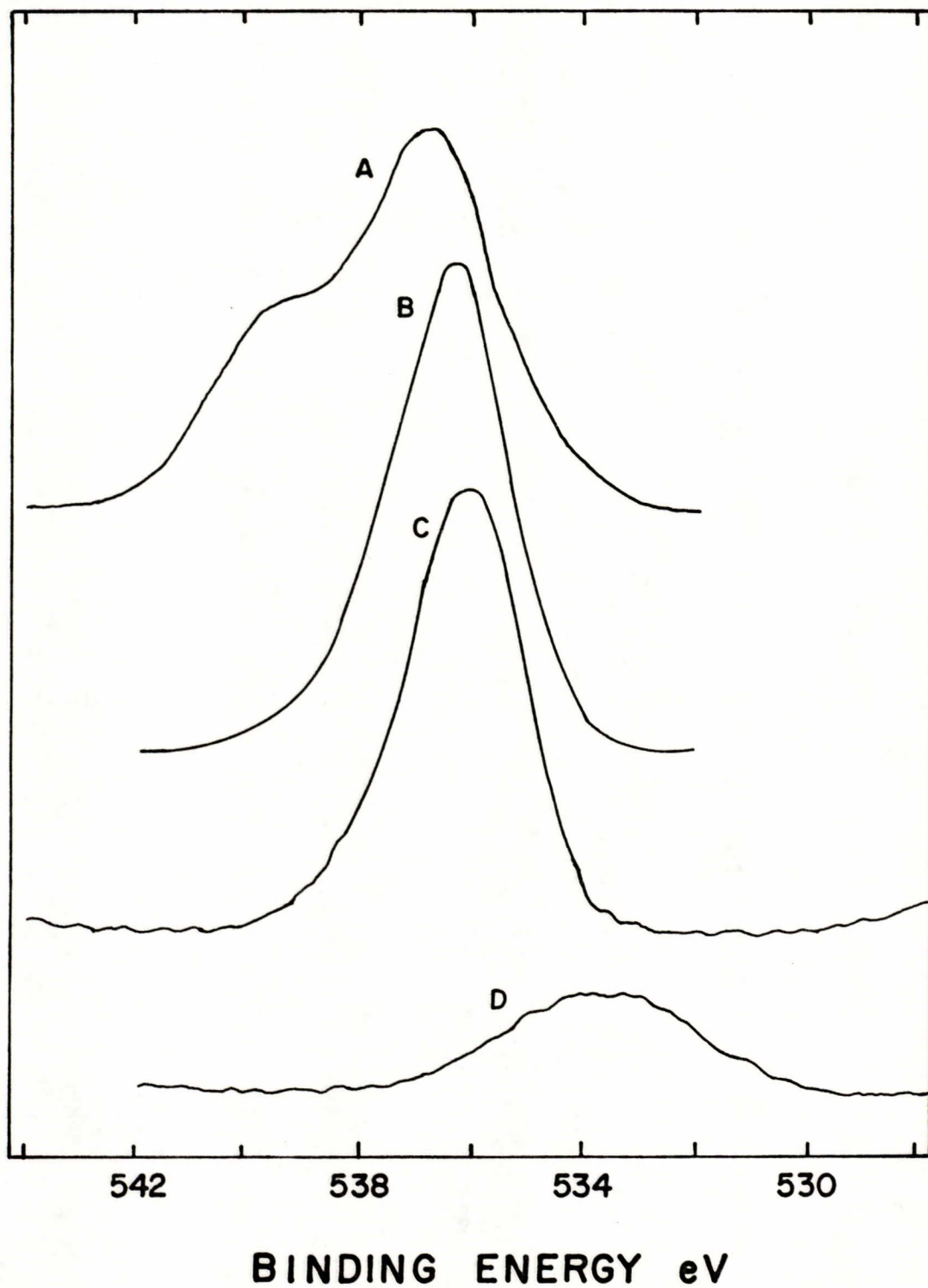
Figure 7. Intercalated Species, M, at an Edge Surface Between Two Layers of Carbon. An oxygen atom, O, double bonded to one of the surface carbon atoms is also shown.

Figure 8. Evolution of Carbon Monoxide. A: Sigma and pi bonds between an oxygen (Ox) and a carbon atom. The dotted lines represent pi electron clouds in the carbon layer. B: Intercalated potassium (K) provides extra electrons to form the second pi bond between carbon and oxygen atoms. C: Removal of carbon monoxide molecule.





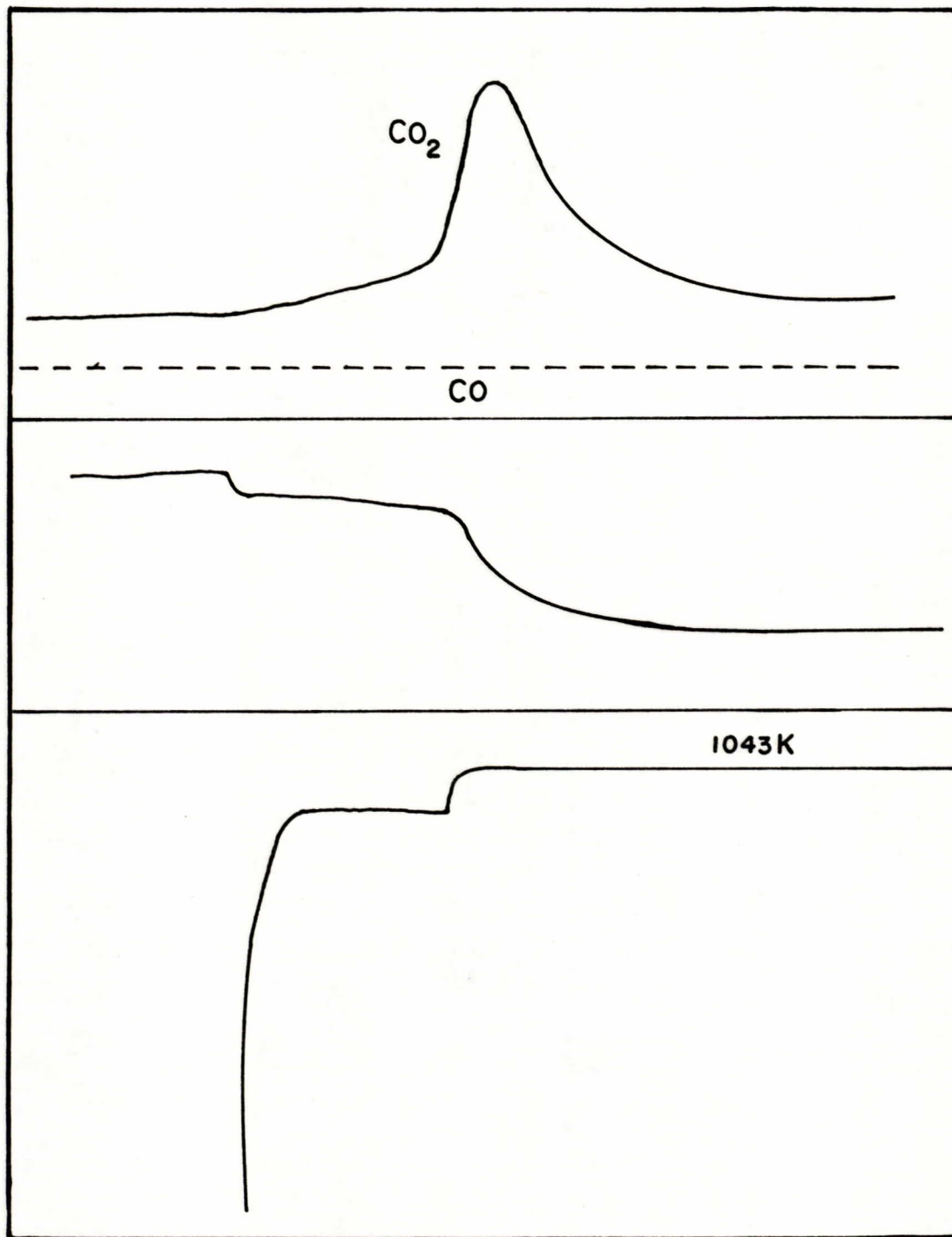
RELATIVE INTENSITY



TEMPERATURE

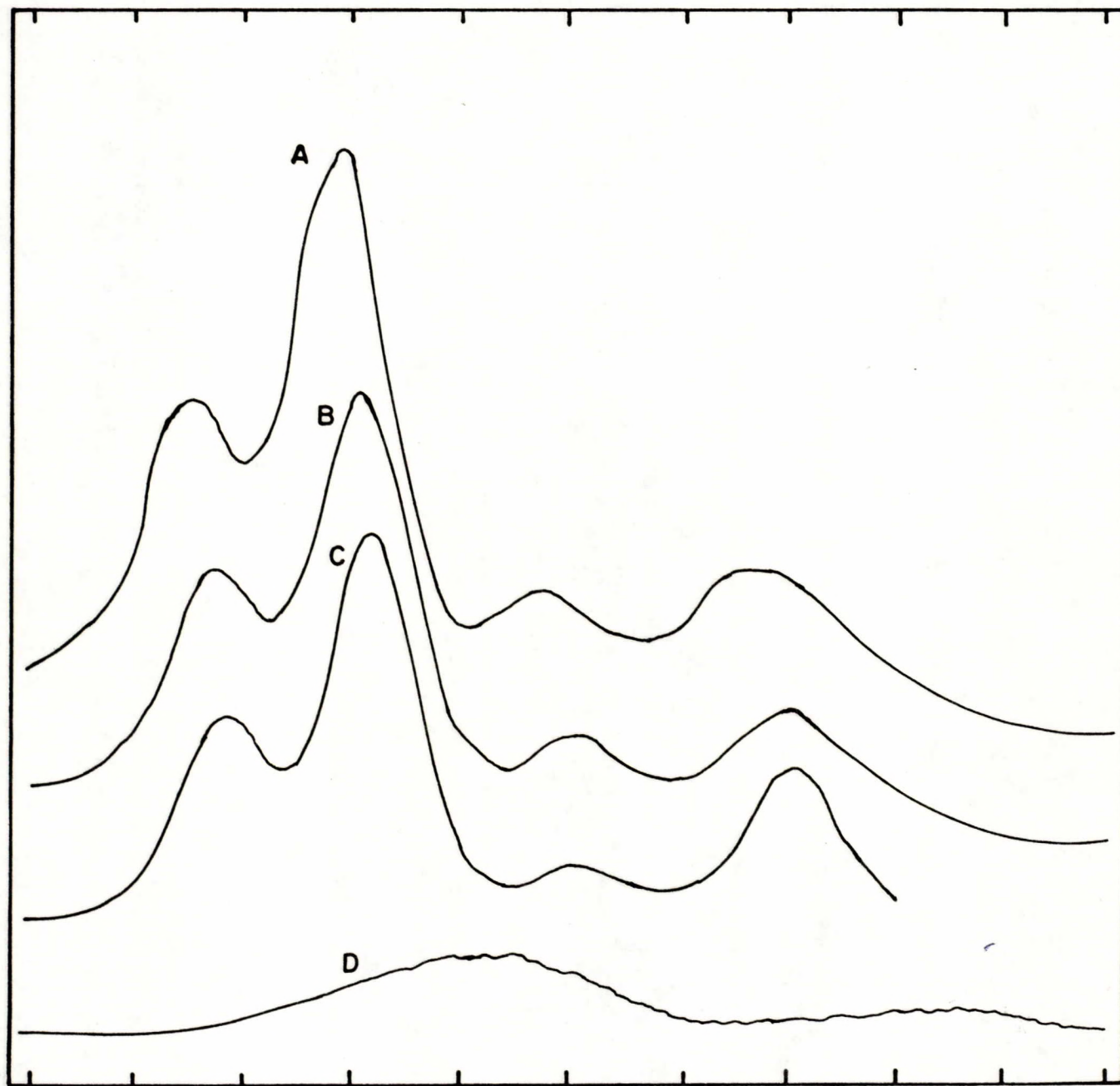
WEIGHT

GAS CONCENTRATION



REACTION TIME

RELATIVE INTENSITY



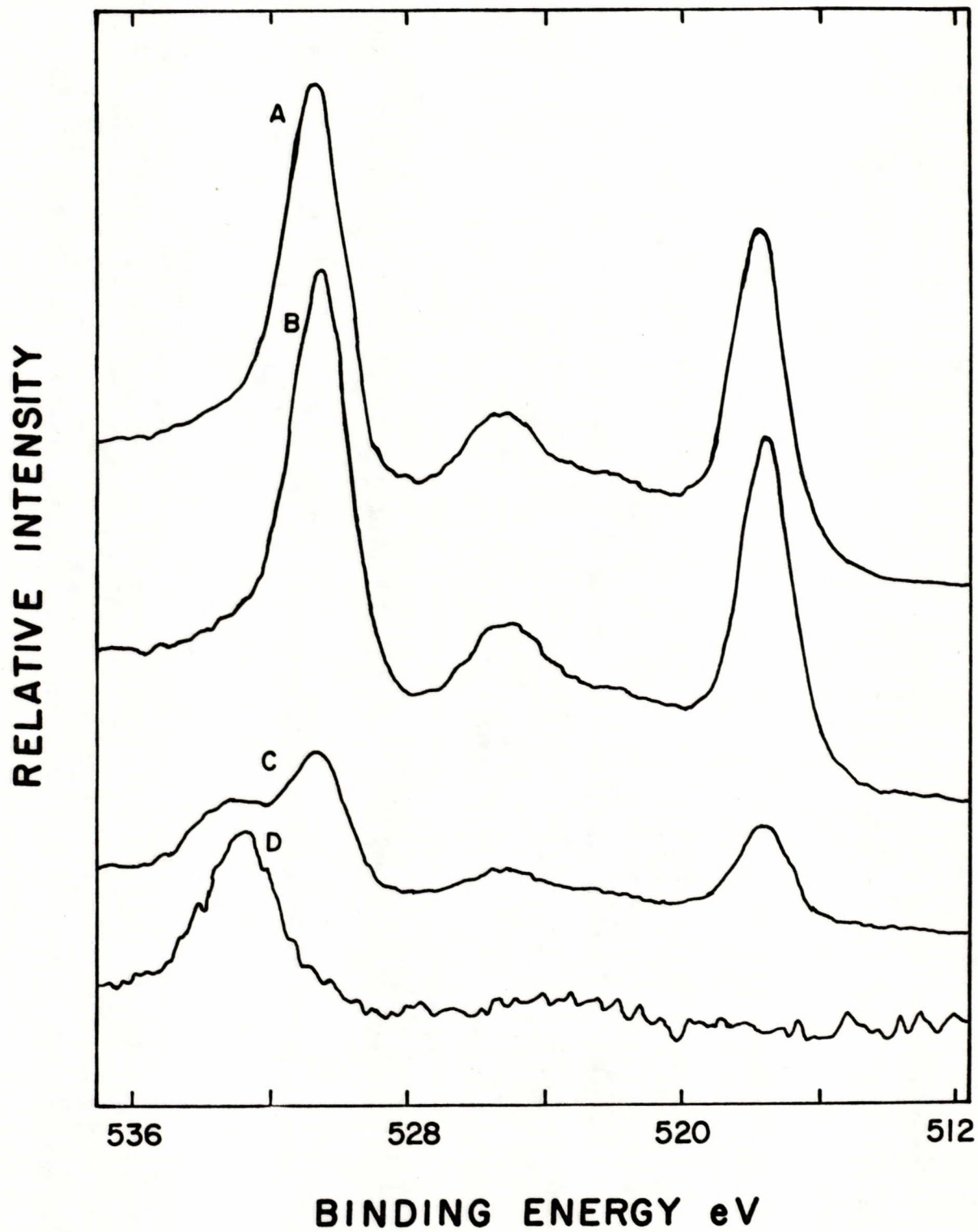
300

296

292

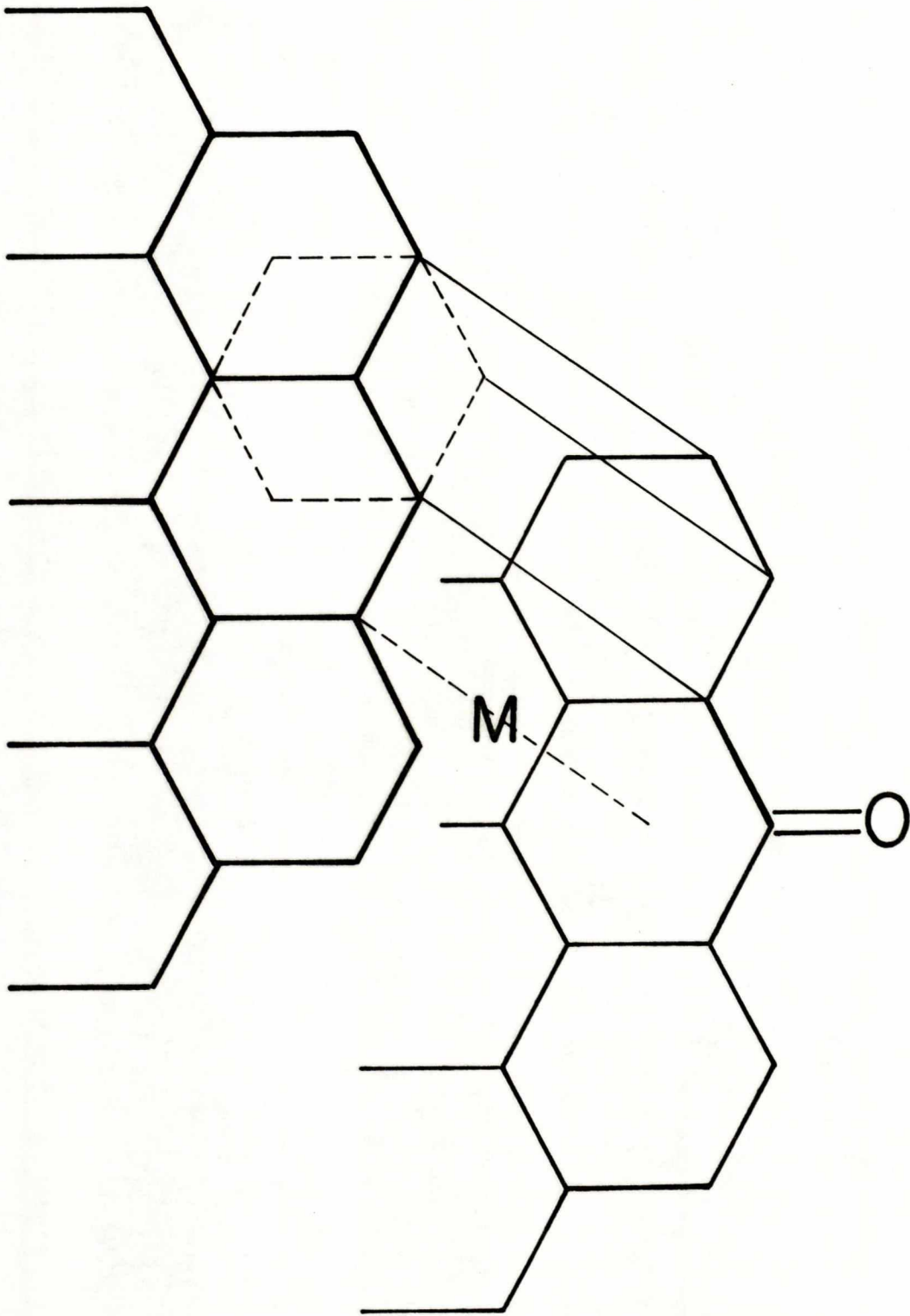
288

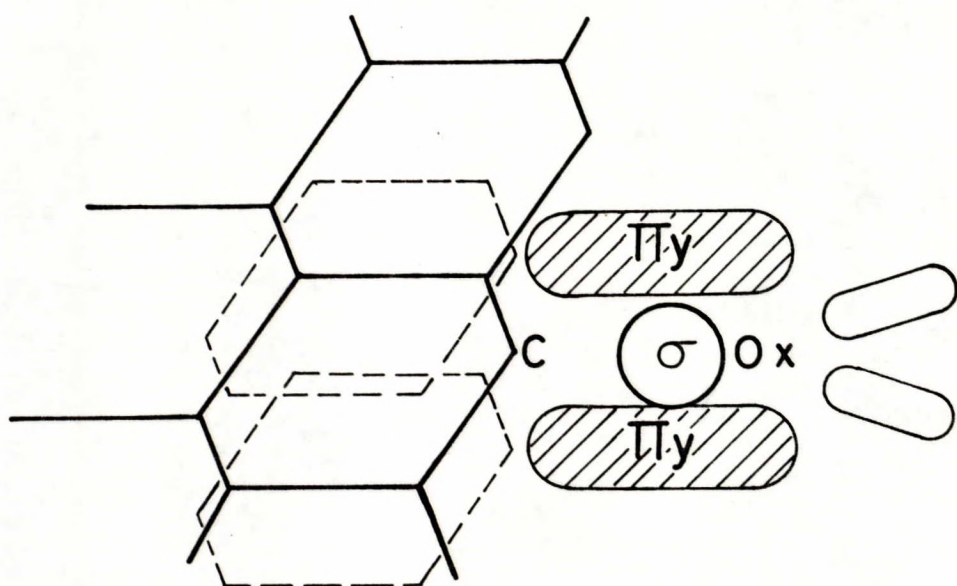
BINDING ENERGY eV



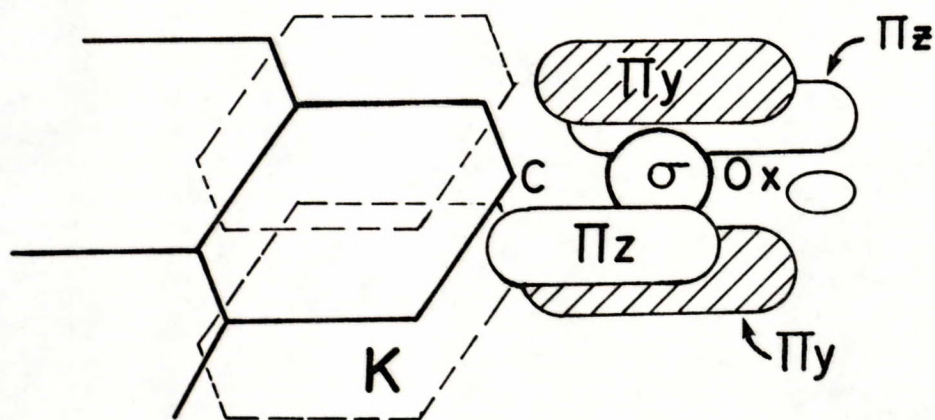
TERHAR + TERHAR

Fig 6

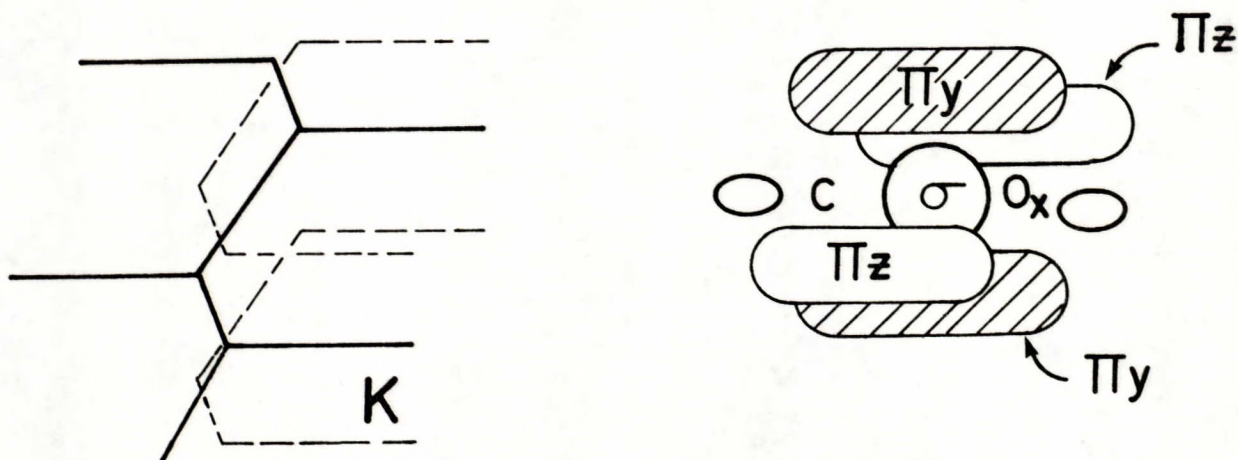




A



B



C